

SUPPLEMENTARY MATERIAL

Table of contents

Supplementary Methods

Supplementary Figures

Supplementary Figure 1

Supplementary Figure 2

Supplementary Figure 3

Supplementary Figure 4

Supplementary Figure 5

Supplementary Figure 6

Supplementary Table

Supplementary References

Supplementary Methods

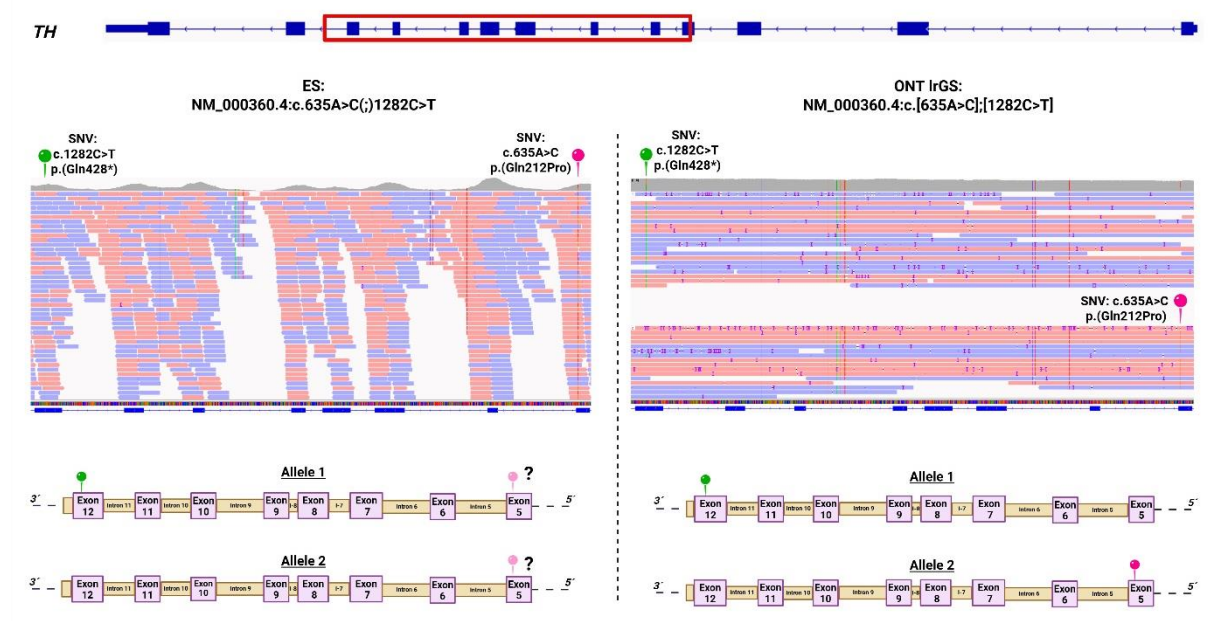
Variant analysis in ONT data

The following packages were deployed with default parameters for the study of different variant types and DNA-base modifications in aligned ONT IrGS BAM files: the diploid variant calling program Clair3 v1.0.4 (<https://github.com/HKU-BAL/Clair3>) for detection of SNVs and indels; Spectre v0.2 (<https://github.com/fritzsedlazeck/Spectre>) for identification of CNVs; Sniffles2 v2.4 (<https://github.com/fritzsedlazeck/Sniffles>) for discovery of other SVs including cxSVs; straglr v1.4.5 (<https://github.com/bcgsc/straglr>) for TRE genotyping; and modkit v0.4 (<https://github.com/nanoporetech/modkit>) for scrutiny of CpG methylation marks in selected samples for which assaying CpG methylation was considered useful for data interpretation. We called variants of interest by the respective software and confirmed disease-causing alterations visually by using the Integrative Genome Viewer (IGV)¹. Variants were phased by implementing the haplotype phasing tool “Whatshap” (<https://whatshap.readthedocs.io/en/latest/>) and by selecting the “Group alignments by: phase” option in IGV. Coordinates of SV breakpoints were determined by visual inspection of read alignments and human BLAT tool searches. TRE analysis was carried out at the locus of interest and repeat patterns were visually assessed based on the aligned reads using IGV. The missing variants in two patients were identified by searching the variant-output files provided by Clair3 and Spectre for mutational changes of genes associated with the suspected clinical differential diagnosis. Methylation profiles were highlighted in IGV by coloring alignments by modified bases. In the context of a *KMT2B* variant, we evaluated methylation information at 80 CpG sites that had been identified to contribute to the definition of a *KMT2B*-related dystonia-specific episignature through previous microarray experiments². More specifically, methylation data used in the downstream analysis were obtained from aligned ONT IrGS BAM files with the help of modkit. We followed recently published principles and recommended approaches to determine the similarity between ONT IrGS- and array-based episignatures for mutant *KMT2B* (see reference³). Methylation data were extracted from ONT data at pre-defined episignature CpG sites (n=80, see Suppl.Fig.4) using GRCh38/hg38 coordinates. Hierarchical clustering analysis and support-vector machine (SVM) development were undertaken, as previously reported²⁻⁵. Following SVM training, SVM-based analysis was performed to predict the presence of a *KMT2B*-specific episignature in patient-14, considering 37 control-subject samples and four samples from dystonia-affected individuals without *KMT2B* rare variants as reference.

Variant confirmation was carried out as appropriate. All variations were visually confirmed by direct parallel manual assessments in annotated SRS and ONT IrGS data. Exact breakpoint locations of each SV were determined based on IGV visualizations¹. SNV/indel and simple small CNV events were confirmed with Sanger sequencing. Larger SVs/cxSVs and TREs were validated using combinations of qPCR, SNP array-based methods, or other PCR-based techniques including conventional amplification of breakpoints with follow-up Sanger analysis and/or fragment length analysis⁶⁻⁸. Conventional *KMT2B* episignature testing was also performed for validation². Validations of SVs and TREs were carried out in external accredited laboratories⁸.

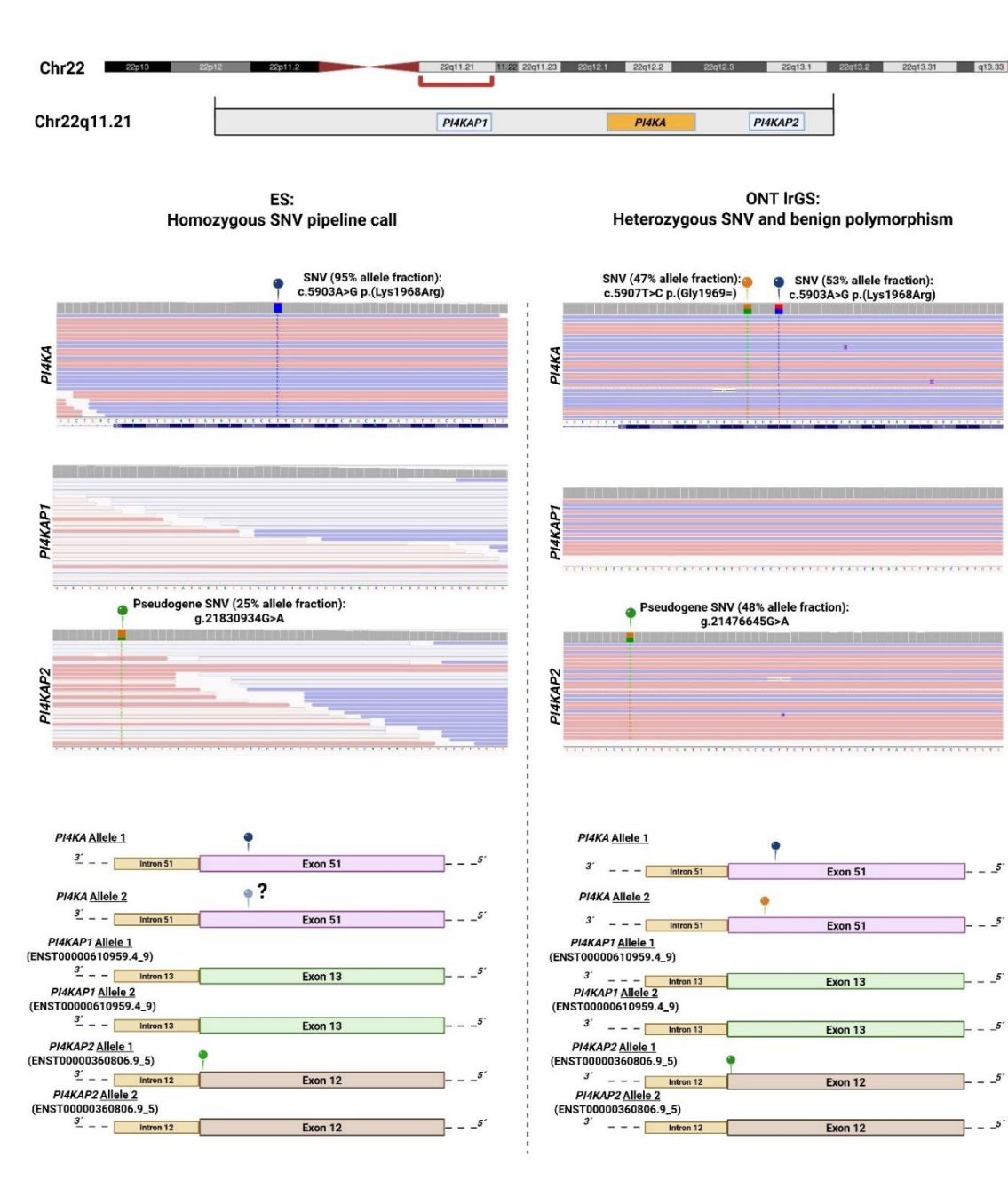
Supplementary Figures

Suppl. Figure 1 Successful variant phasing performed on patient-3



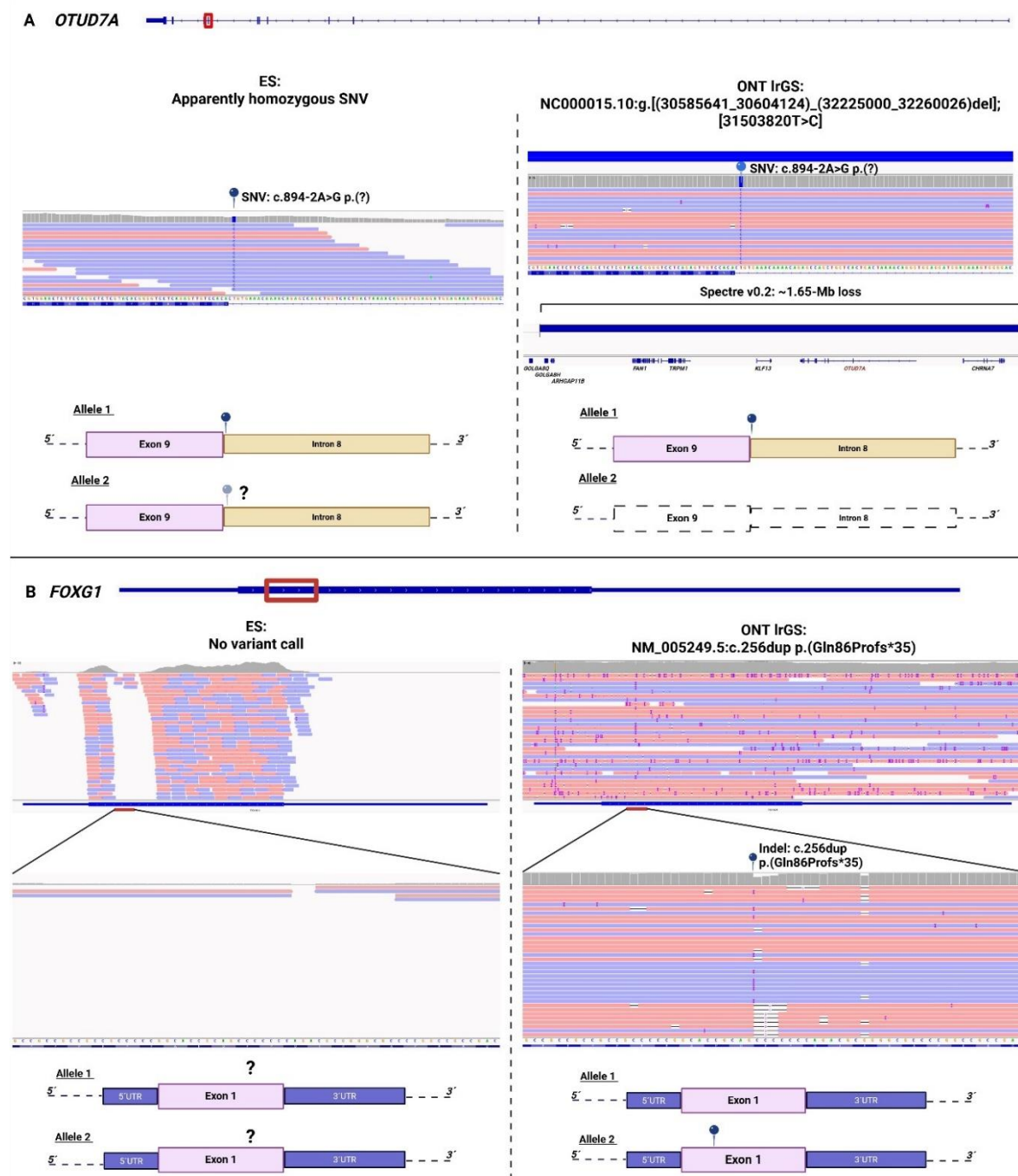
Visualizations of genomic alignments of previously acquired ES data^{6,8} and herein-produced ONT IrGS data in the IGV software¹ are shown. ES variant annotations were based on genome assembly GRCh37/hg19^{6,8}, while ONT IrGS data were analyzed using GRCh38/hg38. Relevant parts of the canonical transcript of the analyzed gene are illustrated at the top of the comparison between ES and ONT IrGS outcomes. IGV zoom-in regions highlight the called variants, which are described according to HGVS nomenclature. Schematic representations of the allelic configurations before and after resolution by LRS are depicted. Alignments are phased into separate haplotypes to determine that the two variants were in *trans*, establishing a compound heterozygous diagnosis related to *TH* in patient-3. ES, exome sequencing; HGVS, Human Genome Variation Society; IGV, Integrative Genomics Viewer; LRS, long-read sequencing; ONT IrGS, Oxford Nanopore Technologies-based long-read genome sequencing; SNV, single-nucleotide variant.

Suppl. Figure 2 Resolution of pseudogene-associated read misalignment with a false-positive variant call in patient-11



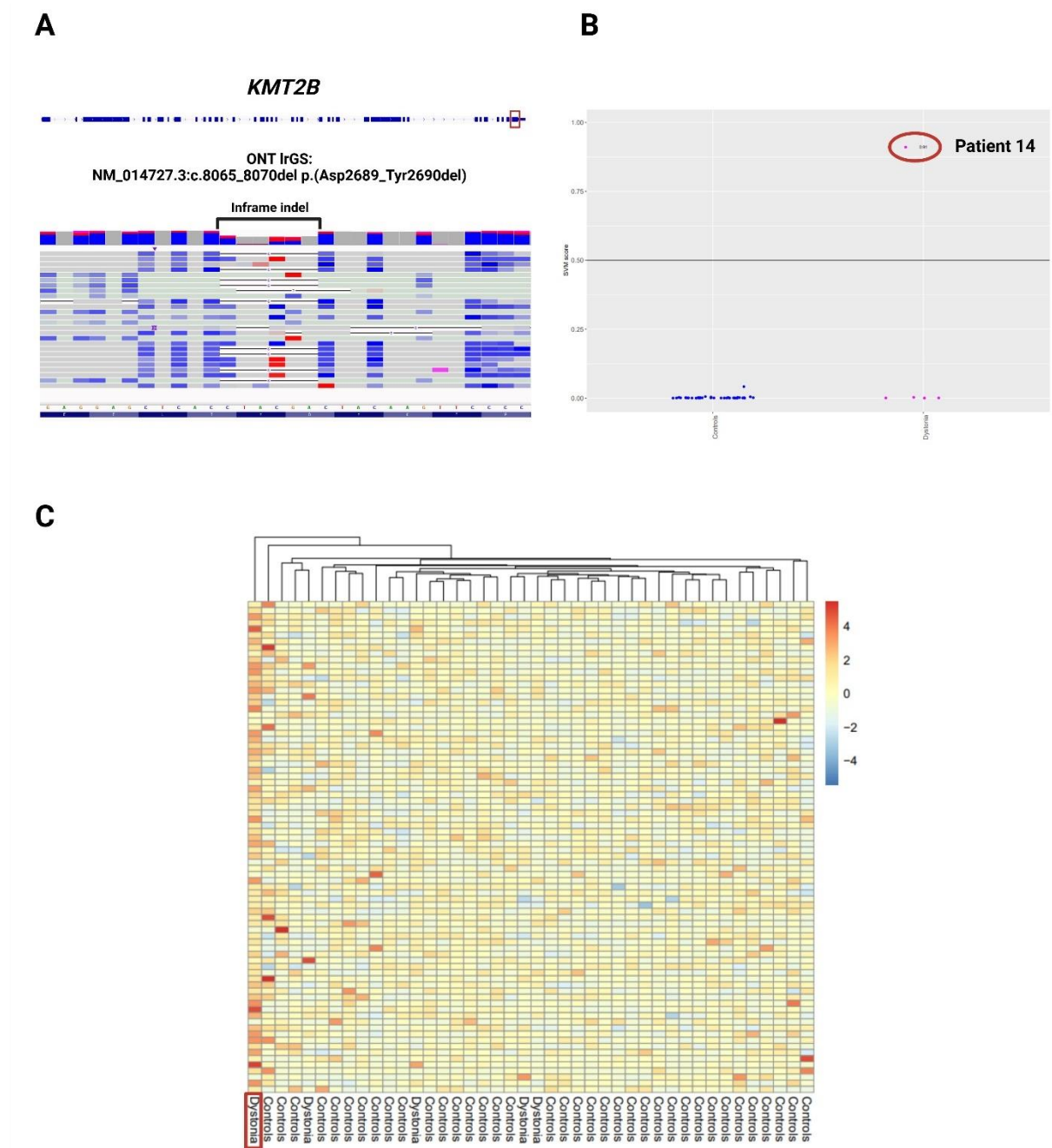
Visualizations of genomic alignments of previously acquired ES data^{6,8} and herein-produced ONT IrGS data in the IGV software¹ are shown. ES variant annotations were based on genome assembly GRCh37/hg19^{6,8}, while coordinates provided for ONT IrGS data refer to GRCh38/hg38. A chromosomal ideogram of the 22q11.21 region containing *PI4KA* and its two pseudogenes *PI4KAP1* and *PI4KAP2* is illustrated at the top of the comparison between ES and ONT IrGS outcomes. IGV zoom-in regions highlight the called variants, along with their read-based variant allele fractions. Schematic representations of the allelic configurations before and after resolution by LRS are depicted. Misalignment of *PI4KA* reads caused by a rare missense substitution in combination with a synonymous polymorphism resulted in a false-positive homozygous variant call in the ES pipeline, which was initially considered a disease-related candidate for patient-11. ONT IrGS mapped the reads to the correct positions and invalidated the homozygous candidate *PI4KA* alteration. ES, exome sequencing; IGV, Integrative Genomics Viewer; LRS, long-read sequencing; ONT IrGS, Oxford Nanopore Technologies-based long-read genome sequencing; SNV, single-nucleotide variant.

Suppl. Figure 3 Missing variants in patients 12 and 13 identified by direct inspection of LRS data



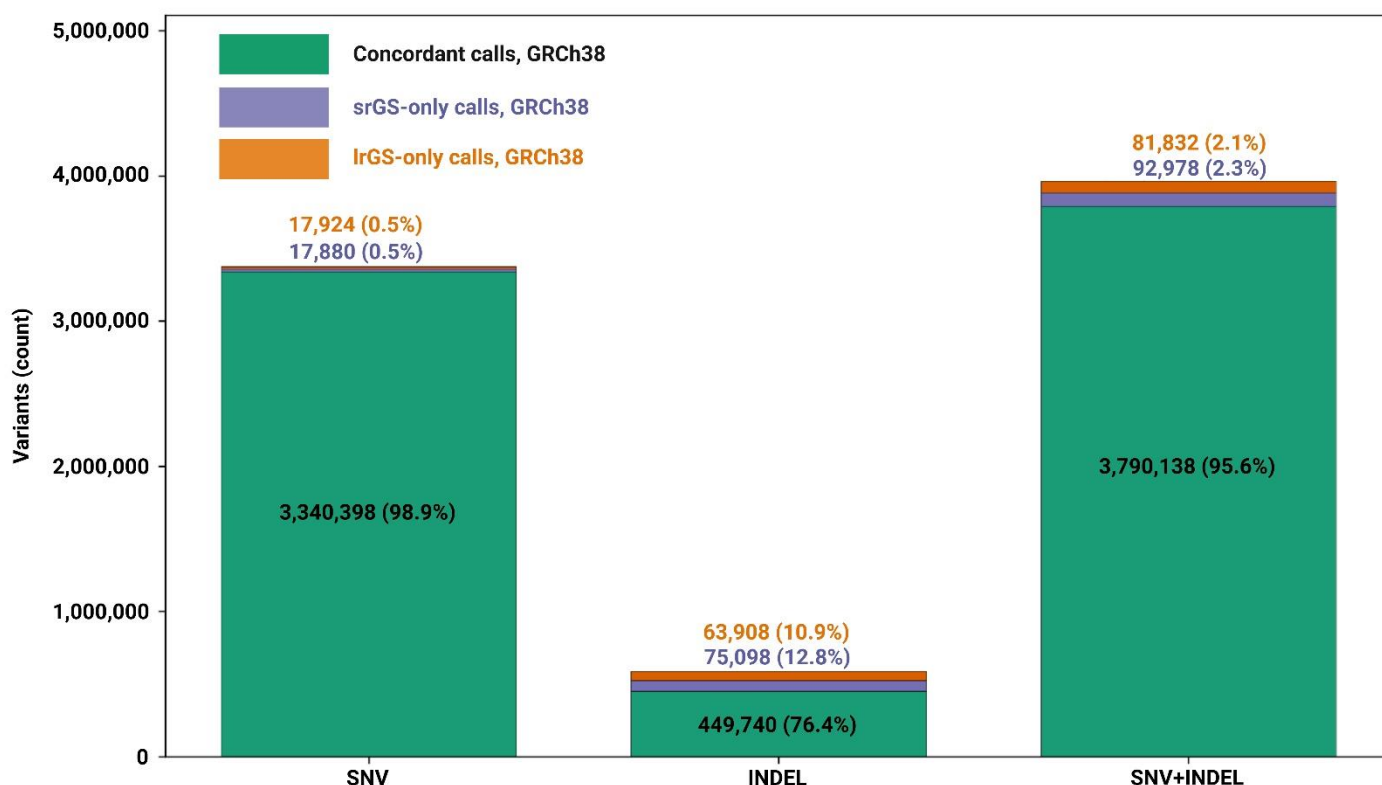
Visualizations of genomic alignments of previously acquired ES data^{6,8} and herein-produced ONT IrGS data in the IGV software¹ are shown. ES variant annotations were based on genome assembly GRCh37/hg19^{6,8}, while coordinates provided for ONT IrGS data refer to GRCh38/hg38. The transcript (or relevant parts of the transcript) of each analyzed gene are illustrated at the top of each comparison between ES and ONT IrGS outcomes. IGV zoom-in regions highlight the positions with missed variants and the called variants; variants are described according to HGVS nomenclature. Schematic representations of the allelic configurations before and after resolution by LRS are depicted. (A) In patient-12, analysis of ONT IrGS data with different variant callers uncovered a previously undetected larger deletion containing the entire coding sequence of *OTUD7A* in addition to an *OTUD7A* SNV, completing the diagnosis of a rare autosomal recessive neurodevelopmental disorder⁹. (B) In patient-13, ONT IrGS identified a *FOXP1* indel in a GC-rich region without coverage in ES data. ES, exome sequencing; HGVS, Human Genome Variation Society; IGV, Integrative Genomics Viewer; indel, short insertion/deletion; LRS, long-read sequencing; ONT IrGS, Oxford Nanopore Technologies-based long-read genome sequencing; SNV, single-nucleotide variant.

Suppl. Figure 4 Parallel detection of a rare variant in *KMT2B* and methylation at 80 episignature-defining CpG sites in patient-14



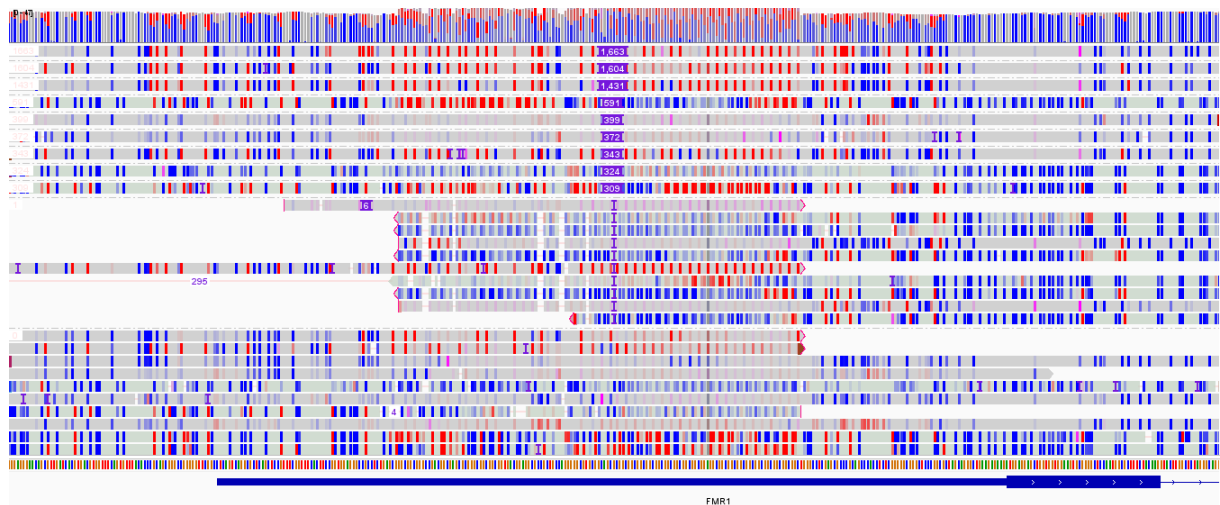
(A) Visualization of genomic alignments of ONT IrGS data in the IGV software¹ is shown. The IGV zoom-in panel highlights the called *KMT2B* indel variant, originally classified as a VUS¹⁰, in patient-14. (B) ONT IrGS-based methylation analysis allowed to distinguish the sample with the *KMT2B* indel from controls (SVM score of 0.91; a score >0.5 indicates that a sample is more likely to bear a disease-related *KMT2B* alteration than not to bear such mutation). ONT IrGS data from 37 control subjects and four dystonia-affected individuals without rare non-synonymous *KMT2B* variants were included in the analysis. The *KMT2B* VUS was subsequently re-classified as likely pathogenic. Methylation patterns at 80 CpG sites that were previously identified to contribute to the definition of a *KMT2B* dystonia-typical episignature² were evaluated. (C) Results from hierarchical clustering analysis based on ONT IrGS data-derived methylation levels (patient-14 with *KMT2B* VUS, 37 control subjects, 4 dystonia-affected individuals without rare non-synonymous *KMT2B* variants). IGV, Integrative Genomics Viewer; indel, short insertion/deletion; ONT IrGS, Oxford Nanopore Technologies-based long-read genome sequencing; SVM, support vector machine; VUS, variant of uncertain significance.

Suppl. Figure 5 Comparison of SNV/indel calls (variations < 50bp) between srGS and ONT IrGS



Breakdown of variant calls (SNVs and indels) that were concordant between srGS (Illumina) and ONT IrGS, or identified by srGS only or by ONT IrGS only. The analysis was conducted with in-house sequencing data produced for a Genome in a Bottle (GIAB) sample¹¹, annotated on GRCh38/hg38, and focused on variants within GIAB's high confidence regions that passed the quality control filter. Indel, short insertion/deletion; ONT IrGS, Oxford Nanopore Technologies-based long-read genome sequencing; SNV, single-nucleotide variant; srGS, short-read genome sequencing.

Suppl. Figure 6 Sorted reads carrying *FMR1* TREs of variable size in patient-9



The suspected mosaic constellation of expanded repeat units is highlighted. *FMR1* methylation is marked in red in the ONT data. Note hypermethylation of long expanded repeats (first four reads). ONT IrGS, Oxford Nanopore Technologies-based long-read genome sequencing; TRE, tandem repeat expansion.

Supplementary Table

Suppl. Table Summary of variant calls (SNVs and indels, < 50bp) produced for a Genome in a Bottle (GIAB) sample¹¹ by srGS and ONT IrGS

Variant type	Total calls (srGS)	Total calls (ONT IrGS)	Concordant calls (srGS-ONT IrGS)	srGS-only calls	ONT IrGS-only calls	Union (srGS, ONT IrGS calls)	Concordance (concordant calls/union)	srGS discordance (srGS-only calls/union)	ONT IrGS discordance (ONT IrGS-only calls/union)
SNV	3358278	3358322	3340398	17880	17924	3376202	0.989395184	0.005295892	0.005308924
INDEL	524838	513648	449740	75098	63908	588746	0.763894787	0.127555856	0.108549357
SNV+INDEL	3883116	3871970	3790138	92978	81832	3964948	0.955911149	0.023449992	0.020638858

The analysis focused on variants within GIAB's high confidence regions that passed the quality control filter. Union = concordant calls (srGS-ONT IrGS) + srGS-only calls + ONT IrGS-only calls.

Indel, short insertion/deletion; ONT IrGS, Oxford Nanopore Technologies-based long-read genome sequencing; SNV, single-nucleotide variant; srGS, short-read genome sequencing.

Supplementary References

1. Robinson JT, Thorvaldsdottir H, Winckler W, et al. Integrative genomics viewer. *Nat Biotechnol* 2011;29(1):24-26.
2. Mirza-Schreiber N, Zech M, Wilson R, et al. Blood DNA methylation provides an accurate biomarker of KMT2B-related dystonia and predicts onset. *Brain* 2021.
3. Geysens M, Huremagic B, Souche E, et al. Clinical evaluation of long-read sequencing-based episignature detection in developmental disorders. *Genome Med* 2025;17(1):1.
4. Oexle K, Zech M, Stuhn LG, et al. Episignature analysis of moderate effects and mosaics. *Eur J Hum Genet* 2023;31(9):1032-1039.
5. Stehr AM, Fischer J, Mirza-Schreiber N, et al. Variable expressivity of KMT2B variants at codon 2565 in patients with dystonia and developmental disorders. *Parkinsonism Relat Disord* 2025;133:107319.
6. Zech M, Jech R, Boesch S, et al. Monogenic variants in dystonia: an exome-wide sequencing study. *Lancet Neurol* 2020;19(11):908-918.
7. Dzinovic I, Boesch S, Skorvanek M, et al. Genetic overlap between dystonia and other neurologic disorders: A study of 1,100 exomes. *Parkinsonism Relat Disord* 2022;102:1-6.
8. Zech M, Dzinovic I, Skorvanek M, et al. Combined genomics and proteomics unveils elusive variants and vast aetiologic heterogeneity in dystonia. *Brain* 2025.
9. Suzuki H, Inaba M, Yamada M, et al. Biallelic loss of OTUD7A causes severe muscular hypotonia, intellectual disability, and seizures. *Am J Med Genet A* 2021;185(4):1182-1186.
10. Richards S, Aziz N, Bale S, et al. Standards and guidelines for the interpretation of sequence variants: a joint consensus recommendation of the American College of Medical Genetics and Genomics and the Association for Molecular Pathology. *Genet Med* 2015;17(5):405-424.
11. Zook JM, McDaniel J, Olson ND, et al. An open resource for accurately benchmarking small variant and reference calls. *Nat Biotechnol* 2019;37(5):561-566.